JOURNAL OF BACTERIOLOGY, Oct. 2010, p. 5465–5471 Vol. 192, No. 20
0021-9193/10/$12.00 doi:10.1128/JB.00613-10

Molecular Basis of Vancomycin Dependence in VanA-Type *Staphylococcus aureus* VRSA-9[▽]

Djalal Meziane-Cherif,[1] Frederick A. Saul,[2] Carole Moubareck,[1] Patrick Weber,[3] Ahmed Haouz,[3] Patrice Courvalin,[1]* and Bruno Périchon[1]

Institut Pasteur, Unité des Agents Antibactériens,[1] Unité d'Immunologie Structurale, CNRS-URA 2185,[2] and Plate-forme 6, CNRS-URA 2185,[3] 25, rue du Docteur Roux, 75724 Paris Cedex 15, France

Received 29 May 2010/Accepted 11 August 2010

The vancomycin-resistant *Staphylococcus aureus* VRSA-9 clinical isolate was partially dependent on glycopeptide for growth. The responsible *vanA* operon had the same organization as that of Tn*1546* and was located on a plasmid. The chromosomal D-Ala:D-Ala ligase (*ddl*) gene had two point mutations that led to Q260K and A283E substitutions, resulting in a 200-fold decrease in enzymatic activity compared to that of the wild-type strain VRSA-6. To gain insight into the mechanism of enzyme impairment, we determined the crystal structure of VRSA-9 Ddl and showed that the A283E mutation induces new ion pair/hydrogen bond interactions, leading to an asymmetric rearrangement of side chains in the dimer interface. The Q260K substitution is located in an exposed external loop and did not induce any significant conformational change. The VRSA-9 strain was susceptible to oxacillin due to synthesis of pentadepsipeptide precursors ending in D-alanyl-D-lactate which are not substrates for the β-lactam-resistant penicillin binding protein PBP2′. Comparison with the partially vancomycin-dependent VRSA-7, whose Ddl is 5-fold less efficient than that of VRSA-9, indicated that the levels of vancomycin dependence and susceptibility to β-lactams correlate with the degree of Ddl impairment. Ddl drug targeting could therefore be an effective strategy against vancomycin-resistant *S. aureus*.

Methicillin-resistant *Staphylococcus aureus* (MRSA) bacteria that have acquired the vancomycin resistance *vanA* operon from glycopeptide-resistant enterococci are designated vancomycin-resistant *S. aureus* (VRSA) (29). Vancomycin acts by binding to the C-terminal acyl-D-Ala-D-Ala of the undecaprenol-diphosphate MurNAc-pentapeptide intermediate and inhibits transglycosylation and transpeptidation reactions in cell wall peptidoglycan polymerization and cross-linking (30). D-Ala-D-Ala is synthesized by the ATP-dependent D-Ala:D-Ala ligase (Ddl) (EC 6.3.2.4) before its incorporation in peptidoglycan precursors (26, 35). VanA-type vancomycin resistance results from the incorporation into peptidoglycan intermediates of a D-alanyl-D-lactate (D-Ala-D-Lac) depsipeptide, synthesized by a D-Ala:D-Lac ligase, which is responsible for diminished binding affinity of glycopeptides for their target. Kinetic analyses of Ddls have established two subsites in the active site for D-Ala binding (24, 27). The reaction mechanism culminates in the transfer of the γ-phosphoryl of ATP to the carboxyl group of D-Ala_1 to produce an acylphosphate and ADP. The acyl carbon atom of the acylphosphate then reacts with the amino group of D-Ala_2 to yield a tetrahedral intermediate. Finally, the intermediate releases phosphate to yield D-Ala-D-Ala.

Mutants of *Enterococcus faecium* (8, 14), *Enterococcus faecalis* (34), and *S. aureus* (23) with an impaired Ddl are able to grow because they use the vancomycin resistance pathway for cell wall synthesis. Since resistance is inducible by the drug, these bacteria require the presence of vancomycin in the culture medium for growth. Ddls from vancomycin-dependent enterococci (14) have mutations affecting amino acids highly conserved in the D-Ala:D-Ala ligase superfamily (10). Molecular modeling based on the X-ray structure of *Escherichia coli* DdlB (11) revealed that all the mutated residues interact directly with one of the substrates of the enzymatic reaction or stabilize the position of critical residues in the active site. However, the degree of enzyme impairment was not evaluated biochemically. Recently, we reported the mechanism of vancomycin dependence in VanA-type *S. aureus* VRSA-7 and showed that the chromosomal Ddl had the single mutation N308K, which probably affects the binding of the transition-state intermediate, leading to a 1,000-fold decrease in activity relative to that of the wild-type enzyme (23). Glycopeptide-dependent mutants could therefore be considered useful tools to explore structure-activity relationships of the Ddl, which represents an attractive target for designing new drugs. Here we describe the partially vancomycin-dependent VanA-type *S. aureus* strain VRSA-9 and report the biochemical and structural characterization of its mutated Ddl.

MATERIALS AND METHODS

Strains, plasmids, and growth conditions. *S. aureus* VRSA-9 was isolated in 2007 from a plantar foot wound (12). *E. coli* Top10 was used as the host in cloning experiments. *E. coli* BL21(DE3)pLys (Novagen, Madison, WI) was used with the pET28a(+) expression vector (Novagen) for production of VRSA-9 Ddl. Strains were grown in brain heart infusion (BHI) broth or agar (Difco Laboratories, Detroit, MI) at 37°C.

Susceptibility testing. Antibiotic susceptibility was tested by disk diffusion on Mueller-Hinton (MH) agar according to the recommendations of the Comité de l'Antibiogramme de la Société Française de Microbiologie (http://www.sfm.asso.fr). MICs of antibiotics were determined by Etest (AB Biodisk, Combourg, France) on MH agar.

* Corresponding author. Mailing address: Unité des Agents Antibactériens, Institut Pasteur, 25, rue du Docteur Roux, 74724 Paris, France. Phone: 33 (0) 1 45 68 83 20. Fax: 33 (0) 1 45 68 83 19. E-mail: patrice.courvalin@pasteur.fr.

▽ Published ahead of print on 20 August 2010.

TABLE 1. Crystallographic parameters and data statistics

Parameter	Result[a]
X-ray data statistics	
Space group	$p2_1\,2_1\,2_1$
Unit cell dimensions (Å)	$a = 84.37$, $b = 87.27$, $c = 91.79$
Data resolution (Å)	43.64–2.30 (2.42–2.30)
No. of unique reflections	29,619 (3,776)
Completeness (%)	96.2 (86.0)
Redundancy	4.5 (3.3)
R_{merge}	0.063 (0.369)
$\langle I/\Sigma(I)\rangle$	16.7 (3.2)
Refinement statistics	
Resolution (Å)	63.25–2.30 (2.33–2.30)
R value (working set)	0.200 (0.233)
R_{free}	0.276 (0.323)
No. of reflections (total)	28,076 (838)
No. of water molecules	272
RMS deviation from ideal	
Bond length (Å)	0.011
Bond angle (°)	1.36
Mean protein B factor value (Å^2)	27.1

[a] Values in parentheses apply to the high-resolution shell.

Contour-clamped homogeneous electric field gel electrophoresis. Pulsed-field gel electrophoresis of genomic DNA embedded in agarose plugs digested with I-CeuI was performed as described previously (6). Fragments generated were hybridized successively to an α-^{32}P-labeled 16S rRNA (*rrs*) probe obtained by amplification of an internal portion of the *rrs* gene (15) and to a *vanA*-specific probe obtained by PCR with the EA1 and EA2 primers (7).

Recombinant DNA techniques. Plasmid DNA isolation, digestion with restriction endonucleases (Amersham Pharmacia Biotech, Uppsala, Sweden), ligation with T4 DNA ligase (Amersham), and transformation of *E. coli* Top10 with recombinant plasmid DNA were performed by standard methods (31).

Production and purification of VRSA-9 Ddl. Oligodeoxynucleotides DdlSABsaI and DdlSAXhoI (23) containing BsaI and XhoI restriction sites, respectively, were used to amplify the *ddl* gene from VRSA-9 with *Pfu* DNA polymerase. The PCR product was cloned in the PCR-blunt vector, sequenced, and subcloned under the control of the T7 promoter in pET28a(+) previously digested with NcoI and XhoI, leading to plasmid pAT521 [pET28a(+)$\Omega ddl_{VRSA\text{-}9}$]. The C-terminal His_6-tagged VRSA-9 Ddl was produced from *E. coli* BL21(DE3)pLys harboring plasmid pAT521. The purified enzyme was stored at −80°C in 50 mM sodium phosphate, pH 7.5, 150 mM KCl (23).

Size exclusion chromatography. Size exclusion chromatography was performed using a Hiload 16/60 Superdex 200 column (GE Healthcare) equilibrated with 50 mM HEPES, pH 7.5, 150 mM KCl, and 1 mM EDTA and eluted in the same buffer at a flow rate of 0.8 ml/min.

Enzyme kinetics. The kinetic parameters of the VRSA-9 Ddl reaction were determined using the ADP release spectrophotometric assay previously described (4, 23, 27). K_m for ATP was measured at a fixed 80 mM concentration of D-Ala. VRSA-9 Ddl was used at a concentration of 1.5 μM.

Analysis of peptidoglycan precursors. Extraction and analysis of peptidoglycan precursors were performed after growth in the absence or in the presence of vancomycin at 8 μg/ml as described previously (22). Results were expressed as the percentage of total late peptidoglycan precursors represented by tetrapeptides, pentapeptides, and pentadepsipeptides determined from the integrated peak areas.

Crystallization, X-ray data collection, processing, and refinement. After unsuccessful attempts to crystallize VRSA-9 Ddl under the conditions reported for crystallization of VRSA-6 (19), crystallization screening was carried out by the vapor diffusion method using a Cartesian nanoliter dispensing system (32). Sitting drops composed of 200 nl of protein at 4 mg/ml in complex with AMPPNP (5′-adenylyl-β,γ-imidodiphosphate) and 200 nl of mother liquor were equilibrated against 150 μl of buffer solution in Greiner plates. Successful results were obtained using ammonium sulfate as a precipitant at concentrations greater than 1.5 M. The best crystals were obtained by the hanging drop method by mixing 1.5 μl of protein solution at 8.6 mg/ml in complex with AMPPNP and 1.5 μl of the reservoir solution containing 2 M ammonium sulfate and 80 mM Tris-HCl, pH 8.5, at 18°C. The crystals appeared within 3 weeks and had dimensions of up to 0.1 mm by 0.1 mm by 0.2 mm. A single crystal of the VRSA-9 Ddl-AMPPNP complex was flash-frozen in liquid nitrogen using a mixture of 50% Paratone and 50% paraffin oil as cryoprotectant. X-ray diffraction data were collected on beamline PROXIMA-1 at Synchrotron SOLEIL (St. Aubin, France). Diffraction images were collected with a rotation of 0.5° per image at a wavelength of 0.9792 Å. The images were integrated with the program XDS (3, 16), and crystallographic calculations were carried out using programs from the CCP4 program suite. The crystal parameters and data statistics are shown in Table 1.

The structure was solved by molecular replacement with the program Phaser (21) as implemented in the CCP4 program package. A single monomer (polypeptide chain B) from the dimeric structure of *S. aureus* Ddl (19) (Protein Data Bank [PDB] 2I87) was used as the search model. A clear molecular replacement solution was obtained for two molecules of VRSA-9 Ddl forming a dimer in the asymmetric unit. This solution corresponds to a solvent content (V_s) of 39.6% with a Matthews coefficient (V_m) of 2.04 Å^3 Da^{-1} (20). The structure of the complex was refined by alternate cycles of restrained maximum-likelihood refinement using the program Refmac5 (28), and manual adjustments were made to the model with Coot (9). The final refinement statistics and model parameters are shown in Table 1. All structural figures were generated using PyMol (5).

Protein structure accession number. Atomic coordinates and structure factors have been deposited in the Protein Data Bank under PDB ID no. 3N8D.

RESULTS AND DISCUSSION

Characterization of VRSA-9. VRSA-9 was resistant to vancomycin (MIC, >256 μg/ml) and teicoplanin (MIC, 16 μg/ml) and was susceptible to oxacillin (MIC, 2 μg/ml). The organization of the *vanA* gene cluster determined by PCR mapping (2) was identical to that of the *vanA* operon in Tn*1546*, and the fragments had the expected size. The *vanA* gene cluster in VRSA-9 was found by contour-clamped homogeneous electric field gel electrophoresis to be located on a plasmid (data not shown). Attempts to transfer VanA-type resistance from VRSA-9 to *E. faecalis* JH2-2, *E. faecium* 64/3, and *S. aureus* BM4602 by conjugation were unsuccessful. Determination of antibiotic susceptibility of VRSA-9 by disc diffusion showed enhanced growth surrounding the vancomycin or teicoplanin disc (Fig. 1), suggesting that the strain was partially dependent on glycopeptide for growth. This was confirmed by growth in liquid medium where the strain grew faster in the presence of 8 μg/ml vancomycin (data not shown).

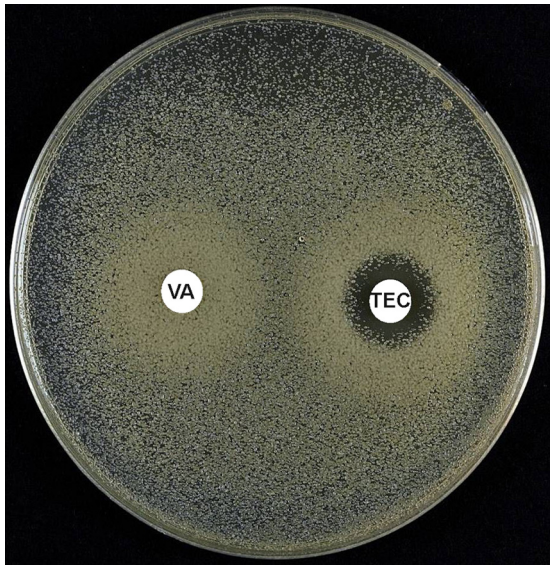

FIG. 1. Glycopeptide dependence of VRSA-9 as tested by disk diffusion. VA, vancomycin; TEC, teicoplanin.

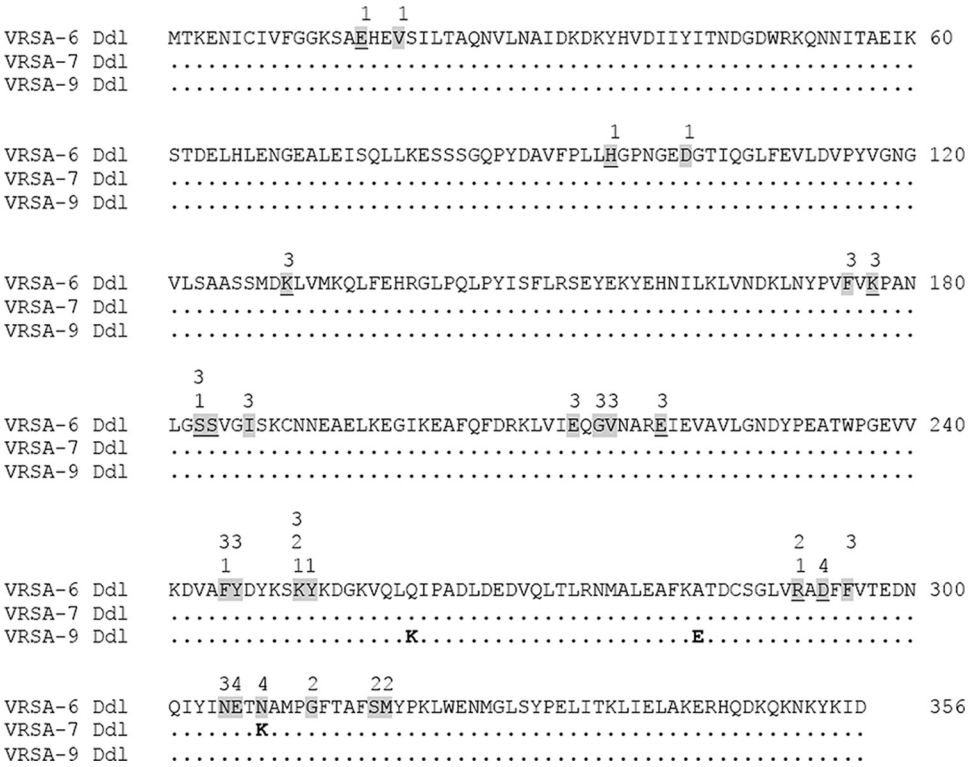

FIG. 2. Sequence alignment of VRSA-9, VRSA-6, and VRSA-7 Ddls. Dots indicate identical amino acids; active-site residues are highlighted in dark gray; underlined residues are conserved in all D-Ala:D-X ligases; amino acid substitutions in VRSA-7 and VRSA-9 Ddls are indicated in bold. Numbering above the sequences indicates amino acids interacting with ligands (1, D-Ala$_1$; 2, D-Ala$_2$; 3, ATP; 4, Mg^{2+}).

Sequence of the VRSA-9 *ddl* gene. It has been shown previously that mutations in the host Ddl of Van-type-resistant enterococci or staphylococci can be responsible for total or partial vancomycin dependence (23, 34). Comparison of the deduced sequence of the *ddl* gene from VRSA-9 with the sequence of that of VRSA-6 (Fig. 2) revealed two amino acid substitutions, Q260K and A283E, resulting from point mutations at nucleotide positions 778 and 848, respectively. The residues at these positions are not conserved among D-Ala:D-Ala ligases and do not interact directly with the substrates (Fig. 2). This type of mutation has been rarely studied by site-directed mutagenesis, as opposed to those which are directly involved in catalytic activity.

Expression of the *vanA* gene cluster. To determine the level of expression of the *vanA* operon in VRSA-9, the nature and relative amounts of cytoplasmic peptidoglycan precursors were determined after growth in the presence (8 μg/ml) and absence of vancomycin in the culture medium. In the absence of vancomycin, VRSA-9 synthesized precursors ending in D-Ala-D-Lac (72%) and D-Ala-D-Ala (21%) (Table 2), suggesting that the host ligase remained partially functional and/or that the VanA ligase can synthesize D-Ala-D-Ala. The presence of tetrapeptide (7%) and pentadepsipeptide in the absence of glycopeptide is most likely due to loose regulation of the *vanA* operon by the VanR/VanS two-component regulatory system (1, 23). After induction, no pentapeptide precursors were detected and pentadepsipeptides represented 90% of the precursors. Since β-lactam susceptibility in VRSA strains is due to synthesis of pentadepsipeptides, which are not substrates for PBP2′ (23, 29), the levels of susceptibility to oxacillin correlate with the nature and the amounts of cytoplasmic cell wall precursors. Accordingly, the MIC of oxacillin against VRSA-9 (2 μg/ml) was significantly higher than that against VRSA-7 (0.025 μg/ml) (23).

Purification and kinetic characterization of VRSA-9 Ddl. The 41-kDa C-terminal His_6-tagged VRSA-9 Ddl was obtained in a soluble form and was more than 99% pure, as determined by SDS-PAGE analysis (data not shown). Using size exclusion chromatography, VRSA-9 Ddl was eluted as a dimer of 82 kDa without any trace of the monomer. A noteworthy property of VRSA-9 Ddl was a lag period in the enzymatic assay (Fig. 3A), a phenomenon not seen in VRSA-6 Ddl or in any other D-Ala:D-X ligase (4, 23, 27). This kinetic behavior is characteristic of hysteretic enzymes which, during catalysis, slowly convert from one kinetic form to another as a

TABLE 2. Cytoplasmic peptidoglycan precursors in extracts from VRSA-9

Induction	Peptidoglycan precursor (%)[a]		
	UDP-MurNAc-tetrapeptide	UDP-MurNAc-pentapeptide [D-Ala]	UDP-MurNAc-pentadepsipeptide [D-Lac]
Uninduced	7	21	72
Vancomycin (8 μg/ml)	10	2	88

[a] The cytoplasmic peptidoglycan precursors of VRSA-9 grown with or without vancomycin were analyzed as described previously (22).

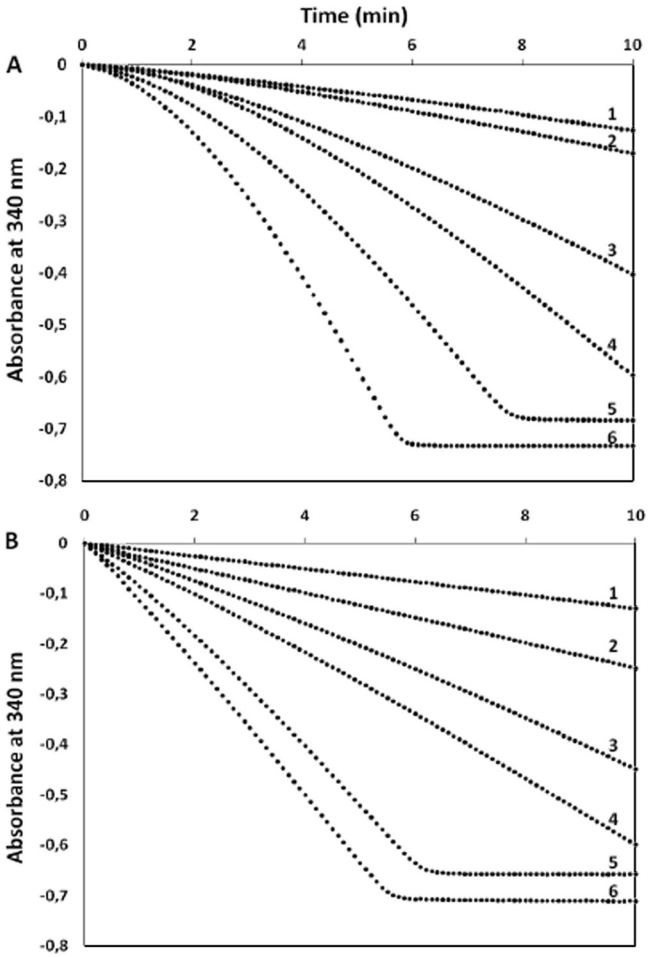

FIG. 3. Comparison of the full time courses of VRSA-9 Ddl reactions at various concentrations of D-Ala (40 to 250 mM) with and without preincubation with ATP. (A) The reaction was initiated by the addition of the enzyme. (B) The reaction was initiated by the addition of D-Ala to the Ddl preincubated for 5 min with 10 mM ATP. Curves 1 to 6 are for 40, 80, 120, 160, 200, and 250 mM D-Ala, respectively.

consequence of ligand binding (13, 25). Indeed, preincubation of the enzyme with ATP for 5 min resulted in the expected time course profile of a conventional nonhysteretic enzyme with an initial linear phase (Fig. 3B). This observation was consistent with the ordered Ter-Ter mechanism of D-Ala:D-Ala ligases where ATP is the first substrate to bind (24). Thus, kinetic constants were determined with VRSA-9 Ddl preincubated with 10 mM ATP for 5 min prior to the addition of the D-Ala substrate. Kinetic analysis indicated that the VRSA-9 Ddl had an altered D-Ala:D-Ala ligase activity relative to that of VRSA-6 with a K_m for D-Ala of 2 mM at subsite 1 and 240 mM at subsite 2 (Table 3). The binding affinity for D-Ala at subsite 2 was 14-fold lower than that of VRSA-6 (23). VRSA-9 Ddl retained noticeable catalytic activity (k_{cat} of 126 min^{-1}) which was only 15-fold lower than that of VRSA-6. Overall, VRSA-9 Ddl was approximately 200-fold less efficient than the VRSA-6 Ddl as indicated by the relative k_{cat}/K_{m2} values (Table 3). The ATP binding affinity of VRSA-9 Ddl was 6 times lower than that of VRSA-6, indicating that the mutations in VRSA-9 Ddl also affected the nucleotide binding site. VRSA-9 Ddl was 5 times more efficient than that of VRSA-7 (23) in D-Ala-D-Ala synthesis, which accounts for the lower levels of vancomycin dependence and susceptibility to β-lactams of the VRSA-9 strain.

Crystal structure of VRSA-9 Ddl. (i) Overall structure. Despite differences in the crystal space group and crystallization conditions, the overall structures of VRSA-9 and VRSA-6 Ddls were very similar. In VRSA-9 Ddl, two monomers formed a homodimer in the crystallographic asymmetric unit, in agreement with the results obtained by size exclusion chromatography, indicating that the A283E and Q260K mutations did not alter the dimeric form of the ligase. The VRSA-9 and VRSA-6 Ddl dimeric structures could be superimposed with an overall root mean square (RMS) deviation of 1.2 Å in alpha carbon positions. As in VRSA-6 Ddl, each monomer was divided into three α/β domains: an N-terminal domain (1 to 120), a central domain (121 to 218), and a C-terminal domain (219 to 356) (19). The mutated residues A283E and Q260K in VRSA-9 Ddl were located in the C-terminal domain, A283E at the dimer interface and Q260K in an exposed external loop (Fig. 4). The electron density maps for the two VRSA-9 Ddl monomers could be traced from residue 2 to 353 for monomer A and from 2 to 358 for monomer B, except for gaps from positions 69 to 72, 96 to 98, 242 to 256, and 354 to 358 in monomer A and from 69 to 73, 96 to 98, 182 to 184, and 246 to 257 in monomer B. These gaps include the ω-loop (peptide region 246 to 256), which plays an important role in substrate binding (11). Gaps were also observed in the ω-loop in the ligand-free, inhibitor-bound, and ADP-Mg^{2+}-bound structures of VRSA-6 Ddl (19) and in ligand-free *Leuconostoc mesenteroides* D-Ala:D-Lac ligase (LmDDl2) (18). Since mutations Q260K and A283E did not induce a global conformational change, the observed 200-fold loss of activity could be due to small rearrangements of

TABLE 3. Kinetic parameters for D-Ala-D-Ala synthesis of VRSA-9 Ddl in comparison with those of VRSA-6 and VRSA-7 Ddls

Ddl	K_{m1}[a] (mM)	K_{m2}[b] (mM)	k_{cat} (min^{-1})	k_{cat}/K_{m2} (min^{-1}/mM)	Relative k_{cat}/K_{m2}	ATP K_m (mM)
VRSA-6[c]	1.2	17	1,925	113	1	0.70
VRSA-7[c]	ND[d]	76.5	7.6	0.1	0.9×10^{-3}	0.86
VRSA-9	2.0	240[e]	126[f]	0.52	4.6×10^{-3}	4.0[g]

[a] K_m at subsite 1.
[b] K_m at subsite 2.
[c] Data from reference 23.
[d] ND, not detectable.
[e] Highest substrate concentration tested.
[f] Activity measured with 15 μg of enzyme (1.3 μM).
[g] Apparent K_m determined with 80 mM D-Ala.

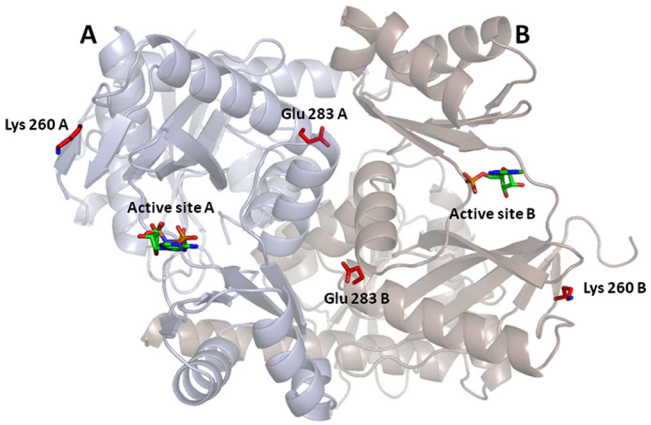

FIG. 4. Overall structure of the VRSA-9 Ddl dimer (monomer A is shown in light blue and monomer B is in light brown). The positions of mutated Lys260 and Glu283 and the nucleotide binding sites are shown. Residue Lys260 is located in an exposed external loop in the C-terminal domain. Residue Glu283 is located near the dimer interface. The overall structure is similar to that of VRSA-6 Ddl (19).

residues involved, either directly or indirectly, in substrate or nucleotide binding. Comparison of the active-site topologies of VRSA-9 and VRSA-6 Ddls and of the environment of the mutations allowed us to identify significant conformational changes that may be responsible for reduced enzymatic activity.

(ii) Effect of mutations Q260K and A283E. Mutation Q260K, in an exposed external loop of the C-terminal domain (Fig. 4), did not induce important conformational changes compared with VRSA-6 Ddl. The A283E mutation resulted in a rearrangement of the side chains of Q135, H139, and E283, leading to new ion-pair interactions and hydrogen bonds in the dimer interface (Fig. 5, panels 1 and 2). In particular, a hydrogen bond was formed between the side chains of H139 and E283 linking the central and C-terminal domains in VRSA-9 Ddl (Fig. 5, panel 1). These interactions, which are different in VRSA-6 Ddl (Fig. 5, panel 2), involved Y147, Q135, E138, H139, E283, and R140 in monomer A and S149, Q135, E138, H139, and E283 in monomer B, resulting in an asymmetric rearrangement in the interface of the dimer. The effect of these structural changes could be propagated throughout the dimeric structure of VRSA-9 Ddl and indirectly affect interactions of catalytic residues with D-Ala substrates or ATP in the active site. Comparison of the VRSA-9 and VRSA-6 Ddl structures showed a shift of the central domain, leading to a more closed conformation of the active site of VRSA-9 Ddl (Fig. 6), which may be responsible for reduced enzymatic activity.

(iii) Ligand binding sites. By analogy with the complexed Ddl structures of DdlB (11), LmDdl2 (18), and TtDdl (17), we could compare the interacting residues in the substrate binding subsites 1 and 2. At subsite 1, the protonated amino group of D-Ala_1 is hydrogen bonded to E16 (VRSA-6 Ddl numbering) and its methyl group is in contact with V19 and H96. At subsite 2, the methyl group of D-Ala_2 makes contact with the side chain of K251 and its carboxylate group interacts with the hydroxyl group of S317 and the main chain nitrogen atom of M318. Residue Y252 in the ω-loop forms a catalytic triad with S183 and E16 and acts to deprotonate the amino group of D-Ala_2, which then makes a nucleophilic attack on the carbonyl atom of the acylphosphate to form a tetrahedral transition-state intermediate. This intermediate is stabilized by interactions with the oxyanion hole formed by the side chain of the strictly conserved residue R291, the side chain nitrogen atom of N308, and the main chain amide of G312 (19).

In the VRSA-9 Ddl structure, the side chains of E16 and V19 are in the same orientation as in VRSA-6 Ddl. Although the electron density of residue H96 was not well defined in the VRSA-9 Ddl crystal structure, we expect the topology of sub-

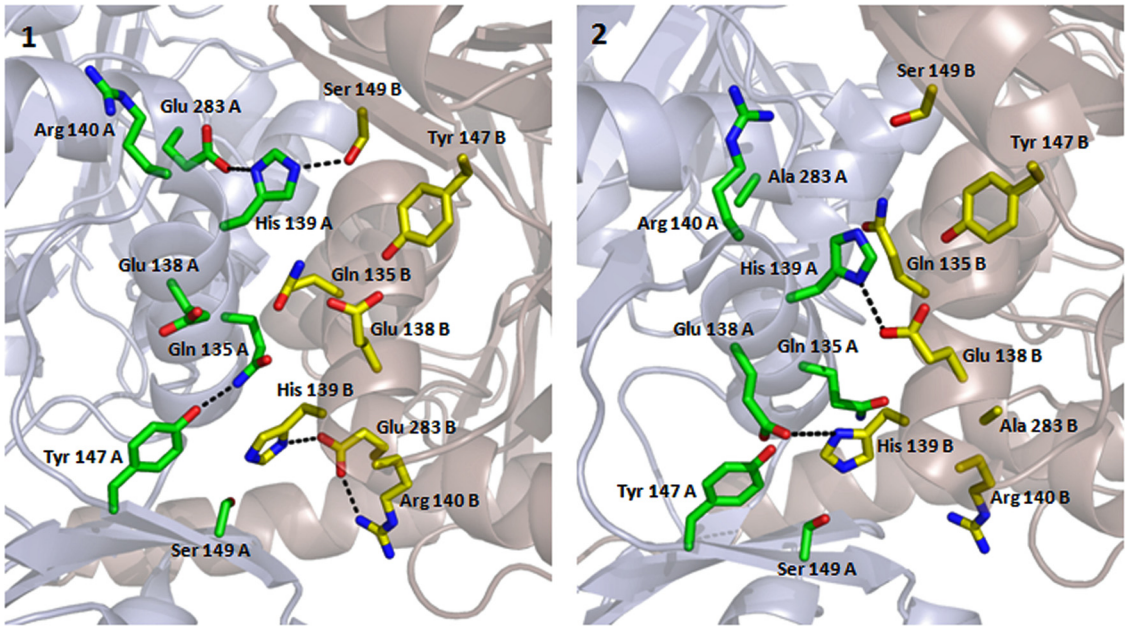

FIG. 5. Detailed view of the dimer interface. (1) VRSA-9 Ddl. (2) VRSA-6 Ddl. Residues in monomer A are shown in green and those in monomer B in yellow. Hydrogen-bonding interactions that differ between the two monomers are shown as dashed lines.

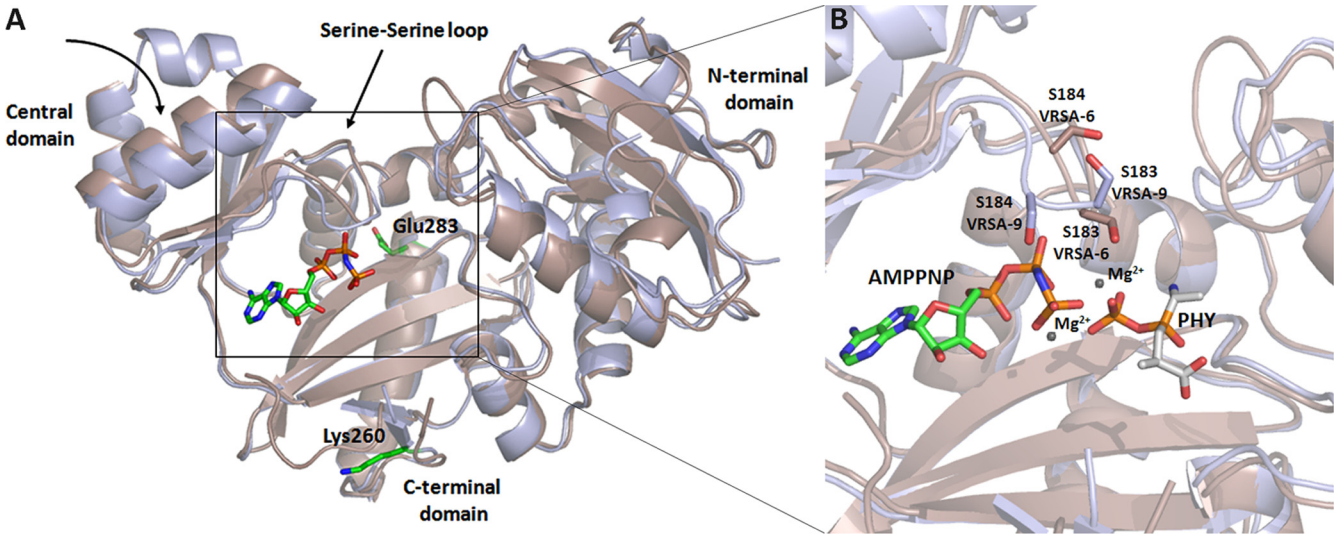

FIG. 6. (A) Superimposed structures of VRSA-9 Ddl (light blue) and VRSA-6 Ddl (light brown) showing the shift of the central domain. (B) Detailed view of the nucleotide binding site and of the serine-serine loop. The phosphoryl phosphinate substrate analog (PHY) was modeled using the structure of LmDdl2 (PDB code 1EHI).

site 1 to be similar to that of VRSA-6 since only slight differences are observed in the affinity for D-Ala_1 (Table 3). At subsite 2, S317 and M318 are conserved, as well as the oxyanion hole formed by R291, N308, and G312. Residue S183, implicated in the catalytic triad, is not visible in the electron density map of VRSA-9 Ddl monomer B, suggesting disorder in the loop between positions 182 and 186. However, in monomer A, the residues S183 and S184 are in opposite orientations in comparison with that of VRSA-6 (Fig. 6). These differences could explain the lower binding affinity of D-Ala_2 which was also observed in *E. coli* DdlB, where the mutation S150A (DdlB numbering) leads to a 53-fold decrease in affinity at subsite 2 (33). Since the ω-loop (peptide region 246 to 256) was not visible in the crystal structures of VRSA-9 and VRSA-6 Ddls, the role of Y252 in the catalytic triad and of the aliphatic chain of K251 could not be determined. VRSA-9 Ddl displayed a 6-fold-lower affinity for ATP than did the wild-type Ddl of VRSA-6 (Table 3). Analysis of the ATP binding site in VRSA-9 Ddl showed that most of the hydrophobic interactions, ion pairs, and hydrogen bonds described in the VRSA-6 Ddl structure (19) are conserved, except for the side chain of S183, which interacts with the β-phosphate of ADP in VRSA-6 Ddl (19). This difference could explain the lower affinity for ATP of VRSA-9 Ddl.

In a recent work (17), the crystal structure of the Ddl from *Thermus thermophilus* HB8 identified four conformational states (open, semiopen, semiclosed, and closed), and the reaction catalyzed by the Ddl is considered to proceed through these states. Upon binding of the substrate, the central domain rotates as a rigid body toward the C-terminal domain. This movement induces a local conformational change in S183 and S184 (VRSA-6 Ddl numbering) and in the ω-loop, resulting in an overall structural change from the open to the closed form. It is possible that the mutation A283E reduces the flexibility of the central domain in VRSA-9 Ddl, leading to lower affinity for ATP and D-Ala. This hypothesis is supported by the observed affinity values of D-Ala_2 and by the hysteretic behavior of VRSA-9 Ddl, where the binding step of ATP is much slower than that in VRSA-6 Ddl. In the crystal structure of VRSA-9 Ddl, some residues critical for enzymatic activity are located in disordered regions, including the ω-loop, the S183-S184 loop in monomer A, and H96 in both monomers. Ideally, one could establish all the steric constraints that may alter VRSA-9 Ddl activity by cocrystallizing the ligase with the phosphinate substrate analog. However, our attempts to cocrystallize VRSA-9 Ddl with the substrate analog have been unsuccessful. This is not surprising given the low substrate binding affinities of VRSA-9 Ddl.

In conclusion, the crystal structure of VRSA-9 Ddl shows the importance of conformational changes in the dimer interface which can indirectly affect the topology of the active site. Comparative analysis of the partially vancomycin-dependent VRSA-9 and VRSA-7 showed that the degree of Ddl impairment is correlated with levels of vancomycin dependence and, consequently, susceptibility to oxacillin. Therefore, Ddl drug targeting could represent an effective therapeutic strategy against VRSA as well as MRSA and other pathogenic bacteria.

ACKNOWLEDGMENTS

We acknowledge SOLEIL for provision of synchrotron facilities and thank the staff of beamline PROXIMA-I for assistance. We thank P. E. Reynolds for critical reading of the manuscript. *S. aureus* strains were obtained through the Network on Antimicrobial Resistance in *Staphylococcus aureus* (NARSA).

REFERENCES

1. **Arthur, M., F. Depardieu, P. Reynolds, and P. Courvalin.** 1996. Quantitative analysis of the metabolism of soluble cytoplasmic peptidoglycan precursors of glycopeptide-resistant enterococci. Mol. Microbiol. **21:**33–44.
2. **Arthur, M., C. Molinas, F. Depardieu, and P. Courvalin.** 1993. Characterization of Tn*1546*, a Tn*3*-related transposon conferring glycopeptide resistance by synthesis of depsipeptide peptidoglycan precursors in *Enterococcus faecium* BM4147. J. Bacteriol. **175:**117–127.
3. **Collaborative Computational Project, Number 4.** 1994. The CCP4 suite: programs for protein crystallography. Acta Crystallogr. D Biol. Crystallogr. **50:**760–763.
4. **Daub, E., L. E. Zawadzke, D. Botstein, and C. T. Walsh.** 1988. Isolation, cloning, and sequencing of the *Salmonella typhimurium ddlA* gene with

purification and characterization of its product, D-alanine:D-alanine ligase (ADP forming). Biochemistry **27:**3701–3708.
5. **DeLano, W. L.** 2002. The PyMol molecular graphics system. DeLano Scientific, San Carlos, CA. http://www.pymol.org.
6. **Depardieu, F., M. G. Bonora, P. E. Reynolds, and P. Courvalin.** 2003. The *vanG* glycopeptide resistance operon from *Enterococcus faecalis* revisited. Mol. Microbiol. **50:**931–948.
7. **Depardieu, F., B. Perichon, and P. Courvalin.** 2004. Detection of the *van* alphabet and identification of enterococci and staphylococci at the species level by multiplex PCR. J. Clin. Microbiol. **42:**5857–5860.
8. **Dever, L. L., S. M. Smith, S. Handwerger, and R. H. Eng.** 1995. Vancomycin-dependent *Enterococcus faecium* isolated from stool following oral vancomycin therapy. J. Clin. Microbiol. **33:**2770–2773.
9. **Emsley, P., and K. Cowtan.** 2004. Coot: model-building tools for molecular graphics. Acta Crystallogr. D Biol. Crystallogr. **60:**2126–2132.
10. **Evers, S., B. Casadewall, M. Charles, S. Dutka-Malen, M. Galimand, and P. Courvalin.** 1996. Evolution of structure and substrate specificity in D-alanine:D-alanine ligases and related enzymes. J. Mol. Evol. **42:**706–712.
11. **Fan, C., P. C. Moews, C. T. Walsh, and J. R. Knox.** 1994. Vancomycin resistance: structure of D-alanine:D-alanine ligase at 2.3 Å resolution. Science **266:**439–443.
12. **Finks, J., E. Wells, T. L. Dyke, N. Husain, L. Plizga, R. Heddurshetti, M. J. Wilkins, J. Rudrik, J. Hageman, J. B. Patel, and C. Miller.** 2009. Vancomycin-resistant *Staphylococcus aureus*, Michigan, USA, 2007. Emerg. Infect. Dis. **15:**943–945.
13. **Frieden, C.** 1979. Slow transitions and hysteretic behavior in enzymes. Annu. Rev. Biochem. **48:**471–489.
14. **Gholizadeh, Y., M. Prevost, F. V. Bambeke, B. Casadewall, P. M. Tulkens, and P. Courvalin.** 2001. Sequencing of the *ddl* gene and modeling of the mutated D-alanine:D-alanine ligase in glycopeptide-dependent strains of *Enterococcus faecium*. Protein Sci. **10:**836–844.
15. **Greisen, K., M. Loeffelholz, A. Purohit, and D. Leong.** 1994. PCR primers and probes for the 16S rRNA gene of most species of pathogenic bacteria, including bacteria found in cerebrospinal fluid. J. Clin. Microbiol. **32:**335–351.
16. **Kabsch, W.** 1988. Evaluation of single-crystal X-ray diffraction data from a position-sensitive detector. J. Appl. Crystallogr. **21:**916–924.
17. **Kitamura, Y., A. Ebihara, Y. Agari, A. Shinkai, K. Hirotsu, and S. Kuramitsu.** 2009. Structure of D-alanine-D-alanine ligase from *Thermus thermophilus* HB8: cumulative conformational change and enzyme-ligand interactions. Acta Crystallogr. D Biol. Crystallogr. **65:**1098–1106.
18. **Kuzin, A. P., T. Sun, J. Jorczak-Baillass, V. L. Healy, C. T. Walsh, and J. R. Knox.** 2000. Enzymes of vancomycin resistance: the structure of D-alanine-D-lactate ligase of naturally resistant *Leuconostoc mesenteroides*. Structure **8:**463–470.
19. **Liu, S., J. S. Chang, J. T. Herberg, M. M. Horng, P. K. Tomich, A. H. Lin, and K. R. Marotti.** 2006. Allosteric inhibition of *Staphylococcus aureus* D-alanine:D-alanine ligase revealed by crystallographic studies. Proc. Natl. Acad. Sci. U. S. A. **103:**15178–15183.
20. **Matthews, B. W.** 1968. Solvent content of protein crystals. J. Mol. Biol. **33:**491–497.
21. **McCoy, A. J., R. W. Grosse-Kunstleve, P. D. Adams, M. D. Winn, L. C. Storoni, and R. J. Read.** 2007. Phaser crystallographic software. J. Appl. Crystallogr. **40:**658–674.
22. **Messer, J., and P. E. Reynolds.** 1992. Modified peptidoglycan precursors produced by glycopeptide-resistant enterococci. FEMS Microbiol. Lett. **73:**195–200.
23. **Moubareck, C., D. Meziane-Cherif, P. Courvalin, and B. Perichon.** 2009. VanA-type *Staphylococcus aureus* strain VRSA-7 is partially dependent on vancomycin for growth. Antimicrob. Agents Chemother. **53:**3657–3663.
24. **Mullins, L. S., L. E. Zawadzke, C. T. Walsh, and F. M. Raushel.** 1990. Kinetic evidence for the formation of D-alanyl phosphate in the mechanism of D-alanyl-D-alanine ligase. J. Biol. Chem. **265:**8993–8998.
25. **Neet, K. E., and G. R. Ainslie, Jr.** 1980. Hysteretic enzymes. Methods Enzymol. **64:**192–226.
26. **Neuhaus, F. C.** 1960. The enzymatic synthesis of D-alanyl-D-alanine. Biochem. Biophys. Res. Commun. **3:**401–405.
27. **Neuhaus, F. C.** 1962. The enzymatic synthesis of D-alanyl-D-alanine. II. Kinetic studies on D-alanyl-D-alanine synthetase. J. Biol. Chem. **237:**3128–3135.
28. **Pannu, N. S., G. N. Murshudov, E. J. Dodson, and R. J. Read.** 1998. Incorporation of prior phase information strengthens maximum-likelihood structure refinement. Acta Crystallogr. D Biol. Crystallogr. **54:**1285–1294.
29. **Perichon, B., and P. Courvalin.** 2009. VanA-type vancomycin-resistant *Staphylococcus aureus*. Antimicrob. Agents Chemother. **53:**4580–4587.
30. **Reynolds, P. E.** 1989. Structure, biochemistry and mechanism of action of glycopeptide antibiotics. Eur. J. Clin. Microbiol. Infect. Dis. **8:**943–950.
31. **Sambrook, J., E. F. Fritsch, and T. Maniatis.** 1989. Molecular cloning: a laboratory manual, 2nd ed. Cold Spring Harbor Laboratory Press, Cold Spring Harbor, NY.
32. **Santarsiero, B. D., D. T. Yegian, C. C. Lee, G. Spraggon, J. Gu, D. Scheibe, D. C. Uber, E. W. Cornell, R. A. Nordmeyer, W. F. Kolbe, J. Jin, A. L. Jones, J. M. Jaklevic, P. G. Schultz, and R. C. Stevens.** 2002. An approach to rapid protein crystallization using nanodroplets. J. Appl. Crystallogr. **35:**278–281.
33. **Shi, Y., and C. T. Walsh.** 1995. Active site mapping of *Escherichia coli* D-Ala-D-Ala ligase by structure-based mutagenesis. Biochemistry **34:**2768–2776.
34. **Van Bambeke, F., M. Chauvel, P. E. Reynolds, H. S. Fraimow, and P. Courvalin.** 1999. Vancomycin-dependent *Enterococcus faecalis* clinical isolates and revertant mutants. Antimicrob. Agents Chemother. **43:**41–47.
35. **Walsh, C. T.** 1989. Enzymes in the D-alanine branch of bacterial cell wall peptidoglycan assembly. J. Biol. Chem. **264:**2393–2396.